Different modulation of phospholipase A_2 activity by saturated and monounsaturated *N*-acylethanolamines

Giovanna Zolese,[1,*] Michal Wozniak,[§] Paolo Mariani,[†] Letizia Saturni,[§] Enrico Bertoli,[*] and Annarina Ambrosini[*]

Istituto di Biochimica* and Istituto di Scienze Fisiche and INFM,† Università di Ancona, 60100 Ancona, Italy; and Department of General Chemistry,§ University of Gdansk, Gdansk, Poland

Abstract The physiological functions of *N*-acylethanolamines (NAEs) are poorly understood, although many functions were suggested for these naturally occurring membrane components of plants and animals. The binding with cannabinoid receptors CB1 and CB2 was demonstrated for some NAEs, such as anandamide. However, the chemical nature of these molecules suggests that some of their biological effects on biomembranes could be related, at least partially, to physical interactions with the lipid bilayer. The present work studies the effect of saturated and monounsaturated NAEs on phospholipase A_2 (PLA_2) activity, which is dependent on lipid bilayer features. The present study, performed by 2-dimethylamino-(6-lauroyl)-naphthalene (Laurdan) fluorescence, demonstrates that the acyl chain length and the presence of a single double bond are crucial for the enzymatic activity modulation by NAEs. In fact, saturated NAEs with 10 carbon atoms don't affect the PLA_2 activity, while NAEs with 12 and 16 carbon atoms largely activate the enzyme. On the other hand, an acyl chain length of 18 carbon atoms, with or without the presence of a double bond, only slightly affects the enzymatic activity. A structural model for NAE-lipid interactions is proposed in order to explain the differences in PLA_2 activity modulation by these fatty acid derivatives.—Zolese, G., M. Wozniak, P. Mariani, L. Saturni, E. Bertoli, and A. Ambrosini. **Different modulation of phospholipase A_2 activity by saturated and monounsaturated *N*-acylethanolamines. *J. Lipid Res.* 2003.** 44: **742–753.**

Supplementary key words PLA_2 activity • 2-dimethylamino-(6-lauroyl)-naphthalene • 6-propionyl-2-(dimethylamino)-naphthalene • X-rays • dipalmitoylphosphatidylcholine • large unilamellar vesicle

N-acylethanolamines (NAEs) are naturally occurring molecules in plants and animals (1). They are usually present in very small amounts in many mammalian tissues and cells (2) and in plasma (3), where they are thought to be bound to serum proteins (3), likely to albumin (4, 5).

Moreover, NAE content is dramatically increased in stress conditions (1), such as in myocardium-infarcted areas (1), glutamate-induced neuronal cytotoxicity (2), cadmium chloride-administered rat testis (6), etc. A great interest in these compounds developed with the discovery that some of these molecules ("endocannabinoids") are endogenous ligands of cannabinoid receptors CB1 and CB2 (7 and references cited therein). An important implication of this discovery is the possibility existing for the development of new drugs with applications similar to those suggested for cannabis (7), such as, for example, alleviation of inflammation and pain, and stimulation of appetite in cancer patients. The endocannabinoids are derivatives of PUFA's ethanolamides (among these, the arachidonic derivative, C20:4, anandamide, is the most known) or the 2-arachydonoyl-glycerol (2-AG). These compounds activate CB1 and CB2 receptors and exhibit many pharmacological actions similar to those exerted by marijuana (7). However, despite the great effort carried out in studies on endocannabinoids, their physiological roles remain elusive. Furthermore, other compounds similar to anandamide, but characterized by saturated or monounsaturated acyl chains, are physiologically present in a large variety of tissues (8). These molecules are thought to be cannabinoid-receptor inactive (7, 8). Some recent works suggested that these NAEs could prolong and enhance anandamide biological activity by preventing its degradation ("entourage effect") (9, 10). This raises the possibility that these compounds could be used therapeutically to affect anandamide actions. Moreover, other

Manuscript received 3 October 2002 and in revised form 20 December 2002.

Published, JLR Papers in Press, January 16, 2003.
DOI 10.1194/jlr.M200395-JLR200

Abbreviations: DPPC, dipalmitoylphosphatidylcholine; GP, generalized polarization; Laurdan, 2-dimethylamino-(6-lauroyl)-naphthalene; LUV, large unilamellar vesicle; Lyso-PC, lysophosphatidylcholine; MLV, multilamellar vesicle; NAE, *N*-acylethanolamine; NCEA, *N*-caprinoylethanolamine; NOEA, *N*-oleoylethanolamine; NPEA, *N*-palmitoylethanolamine; NSEA, *N*-stearoylethanolamine; PL, phospholipid; PLA_2, phospholipase A_2; Prodan, 6-propionyl-2-(dimethylamino)-naphthalene; 3wGP, three-wavelengths GP.

[1] To whom correspondence should be addressed.
e-mail zolese@popcsi.unian.it

roles could be possible for these NAEs: for example, *N*-palmitoylethanolamine (C16:0; NPEA), a shorter and fully saturated analog of anandamide, is known to be accumulated during inflammation and presents some anti-inflammatory (7) and antinociceptive effects (11). NPEA is now engaged in clinical studies on the treatment of chronic lumbosciatalgia and multiple sclerosis (12). Moreover, a neuroprotective role for NAEs in general and for NPEA in particular has been suggested (13).

It was speculated that NAEs could have cytoprotective functions (13) and membrane stabilizing effects (1), and can protect against lipid peroxidation (1), inhibit the acrosome reaction of sea urchin spermatozoa (14), and might act as lipid mediators to modulate PLDα activity in plants (15).

The chemical nature of NAEs and some experimental evidence suggest that some of their biological effects could be related, at least partially, to physical interactions with the lipidic part of the membrane (1, 16, 17). In fact, previous studies on liposomes demonstrated that phospholipid (PL) physico-chemical properties, such as fluidity and phase transitions (16, 17), are affected by NAEs with different acyl chain lengths and unsaturation. Many important physiological membrane functions [such as enzymatic activities, membrane permeability, hormonal response, etc. (18–20)] are modulated by physico-chemical properties of the lipid bilayer. For example, many physiological processes involve changes in the amount of water bound to lipid bilayer (20), which affects, in particular, the membrane interfacial polarity. A possible role for surface polarity is the binding of substances to membrane: for example, membrane surface properties modulation affects the binding of protein kinase C to the membrane as well as its activity in the membrane-bound state (20).

Moreover, it was demonstrated (21) that the products of phospholipase A_2 (PLA_2) hydrolysis affect membrane interfacial polarity, modulating the enzymatic activity.

The aim of this paper is to elucidate the interaction of saturated and monounsatured NAEs with lipid membranes and to study their effects on PLA_2 activity, which is largely dependent on (22–24) structural, physico-chemical, and dynamic properties of the lipid bilayer. PLA_2 activity studies are of general interest because of the increasing evidence of the important roles played by this enzyme in hormone signal transduction, immune events, allergic reactions, ischemia, spermatozoa acrosomal reaction, and in the development of an inflammatory response in the cell, etc. Furthermore, an enhanced local concentration of active PLA_2 was demonstrated in inflammatory tissues (25).

The use of steady-state fluorescence and X-ray diffraction will allow us to characterize NAEs localization in the bilayer and their effects on physico-chemical and structural membrane properties.

For the first time, the effect due to NAEs differing for acyl chain length and unsaturation will be characterized on one-component liposomes of dipalmitoylphosphatidylcholine (DPPC) chosen to compare results obtained with recent papers on PLA_2 activity modulation by lipid surface (21, 24, 26–28). In fact, many details (e.g., the temperature dependence of the enzymatic rate) were cleared in DPPC large unilamellar vesicles (LUVs) so that these vesicles are used as a fairly simple model system for investigating the delicate interplay between the PLA_2 activity and the physicochemical features of lipid bilayers (29, 30). The study of the NAE-DPPC liposomes interaction with PLA_2 could have a practical application for the possible use of these vesicles as drug microcarrier systems. In fact, the possible therapeutic use of NAEs is linked to their vehiculation to tissues (1, 4).

MATERIALS AND METHODS

The fluorescent probes 2-dimethylamino-(6-lauroyl)-naphthalene (Laurdan) and 6-propionyl-2-(dimethylamino)-naphthalene (Prodan) were purchased from Molecular Probes (Eugene, OR). DPPC was obtained from Avanti Polar (St. Louis, MO). NAEs were synthesized as previously described (17): *N*-caprinoylethanolamine (NCEA; with 10 carbon atoms in the chain, C-10), *N*-lauroylethanolamine (C12), NPEA (C16), *N*-stearoylethanolamine (NSEA; C18), and *N*-oleoylethanolamine (NOEA; C18:1). Porcine pancreas PLA_2 (Boheringer, Germany) was dialyzed in water, lyophilized, and stored at −20°C. Enzyme was tested for purity by electrophoresis.

DPPC, Laurdan, and Prodan were dissolved in the proper solvent and stored at −20°C. NAE was dissolved in ethanol immediately before use. Buffer used was 10 mM Hepes, 0.12 M NaCl, 5 mM KCl, and 0.1 mM EDTA buffer (pH 7.4).

Fluorescence measurements

For fluorescence measurements, DPPC LUVs, with or without desired NAE, were prepared by extrusion through 0.1 μm polycarbonate filters 25 times at 55°C using the LiposoFast apparatus. The NAE-DPPC molar ratio was $R = 0.1$ and, in some experiments, $R = 0.01$. When present, the fluorescent probes were added to DPPC up to a final probe-lipid Pi molar ratio of 1:1,000 before the preparation of vesicle. Unlabeled LUVs were used to subtract background contribution to emission. DPPC concentration was assessed by phosphate assay (31). LUVs were diluted to a final concentration of 0.3 mM lipid Pi. PLA_2 concentration (0.5 μM in the sample) was assessed by measuring the absorbance at 280 nm according to Ludescher et al. (32).

Hydrolysis was triggered by 5 mM Ca^{2+} injection in the cuvette containing liposomes and the enzyme at a final volume of 2 ml. Steady-state fluorescence measurements were performed on a Perkin-Elmer LS50 B. Both Laurdan and Prodan spectral features are largely sensitive to the polarity and to the molecular dynamics of solvent dipoles in probe microenvironment (33–35). Since, these parameters are very different in the gel and in the liquid-crystalline phases of PLs, these probes were demonstrated to be able to monitor PL phase changes (33–35).

Laurdan and Prodan emission spectra were obtained, exciting at 340 nm and 359 nm, respectively. Generalized polarization (GP) for Laurdan is related to membrane polarity changes and was calculated from emission spectra by the following equation, according to Parasassi et al. (33, 34):

$$GP = (I_B - I_R)/(I_B + I_R), \qquad \textit{(Eq. 1)}$$

where I_B and I_R were the intensities at 440 nm and 490 nm.

A decrease of GP value represents an increase of bilayer polarity.

Prodan three-wavelengths GP (3wGP) and the probe partition coefficient (Cp) between the bilayer and the buffer were calcu-

lated according to the method introduced by Krasnowska et al. (35).

For these calculations, Prodan emission in buffer was subtracted from the spectrum obtained in membranes. Both spectra were recorded at 38.7°C. Intensities at 420 nm, 480 nm, and 530 nm were measured both in the original spectra and in those obtained from the subtraction of intensity arising from the probe in buffer. 3wGP represents GP values only related to Prodan emission from membranes, with the same significance as Laurdan GP.

For the Cp calculation (35), we used the fluorescence intensities measured on Prodan emission spectrum in membrane at 420 nm (I_1) at 480 nm (I_2) and 530 nm (I_3). The ratio $I_{2W}/I_{3W} = k_{32} = 2.8$ (35) was between the emission intensities at 480 nm and 530 nm, respectively, of Prodan in water. The lifetimes for Prodan in the gel-phase membrane and in water were $\tau_M = 3.98$ ns and $\tau_W = 1.41$ ns, respectively (35). Briefly, Cp was calculated by the formula:

$$Cp = R_M\,[\text{Water}]/[\text{lipids}], \qquad \textit{(Eq. 2)}$$

where $R_M = R_F\,\tau_W/\tau_M$ and $R_F = (I_2\,k_{32} - I_3)/I_3$.

X-ray diffraction

Samples for X-ray diffraction experiments were prepared mixing aliquots of NAEs and DPPC chloroform solutions at the molar ratio $R = 0.1$. The solvent was removed by a gentle nitrogen flux. Samples were kept under vacuum for several hours. The lipid film was rehydrated at 55°C in the same buffer used for fluorescence measurements using a lipid-to-buffer weight ratio of 1:3. The obtained samples were used for X-ray diffraction experiments performed using a powder diffractometer on a Rigaku Denki RV300 rotating anode generator. The samples were located between two mylar windows in a circular hole. Diffraction data were collected at the constant temperature of 38.7°C ± 0.1°C controlled by a circulation thermostat. In each experiment, a number of sharp reflections were observed and their spacings were measured following the usual procedure (36, 37). The high-angle profiles, centered in the $(3–5\ Å)^{-1}$ region of the scattering curves, were analyzed as reported (37) to derive the nature of the lipid short-range conformation. Low-angle diffraction profiles were indexed using equations that define the spacing of reflections for the different symmetry systems usually observed in lipid phases (lamellar, hexagonal, or 3-dimensional cubic lattices). The indexing problem was easy to solve because in no case were extra peaks observed, which can be ascribed to the presence of unknown phases or to crystalline structures. In the present experimental conditions, only a series of low-angle Bragg reflections indexed according to the lamellar one-dimensional symmetry (spacing ratios 1:2:3, etc.) was observed. From the symmetry, the dimension of the unit cell, which in this case corresponds to the total thickness of the lipid bilayer and of a water layer, was derived. In the following, *a* indicates the unit cell dimension, i.e., the distance between the midplane of two opposing lipid bilayers.

RESULTS

Effects of NAEs on DPPC phase behavior

The spectral characteristics of Laurdan, which is particularly sensitive to lipid phase changes, were used for these studies. Laurdan features are due to the extreme sensitivity to polarity and molecular dynamics of solvent dipoles in its environment, which arise from solvent dipolar relaxation processes (33, 34).

Laurdan emission in the bilayer is strictly dependent

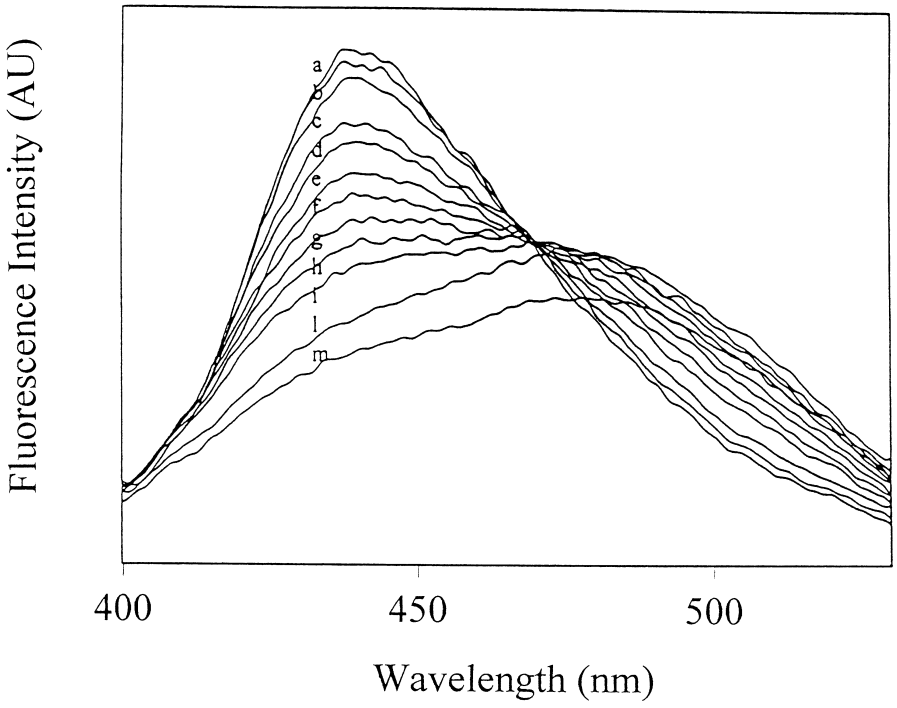

Fig. 1. Steady-state fluorescence emission spectra of 2-dimethylamino-(6-lauroyl)-naphthalene (Laurdan) in dipalmitoylphosphatidylcholine (DPPC) large unilamellar vesicles (LUVs). Samples were suspended in 10 mM Hepes, 0.12 M NaCl, 5 mM KCl, and 0.1 mM EDTA buffer (pH 7.4). Spectra were recorded at λex = 340 nm. Curves: a, 30°C; b, 35°C; c, 38°C; d, 39.3°C; e, 40.2°C; f, 40.6°C; g, 40.8°C; h, 41.3°C; i, 42.4°C; l, 47.4°C; m, 50°C.

from the packing of lipid chains. In a lipid phase below the main phase transition gel phase (τ_M) the emission maximum is near 440 nm, while above the τ_M (liquid-crystalline phase) this maximum is shifted to 490 nm (33). (**Figure 1** shows Laurdan emission spectra recorded in DPPC LUVs at different temperatures.) The steady-state fluorescence parameter GP quantitatively relates the relative fluorescence intensities at 440 nm and 490 nm, and characteristic GP values were shown for gel and liquid crystalline phases (34). These values were demonstrated to be independent from PL headgroups and from pH changes (in the range $4 < pH < 10$). However, the observation of an intermediate GP value is not a final proof of the coexistence of separated PL phase domains, but could indicate homogenous lipid membranes with intermediate polarity between gel and liquid-crystalline phases (38). The GP values measured in PLs undergoing phase changes have been related to the number and motional freedom of water molecules in the probe microenvironment (33, 34).

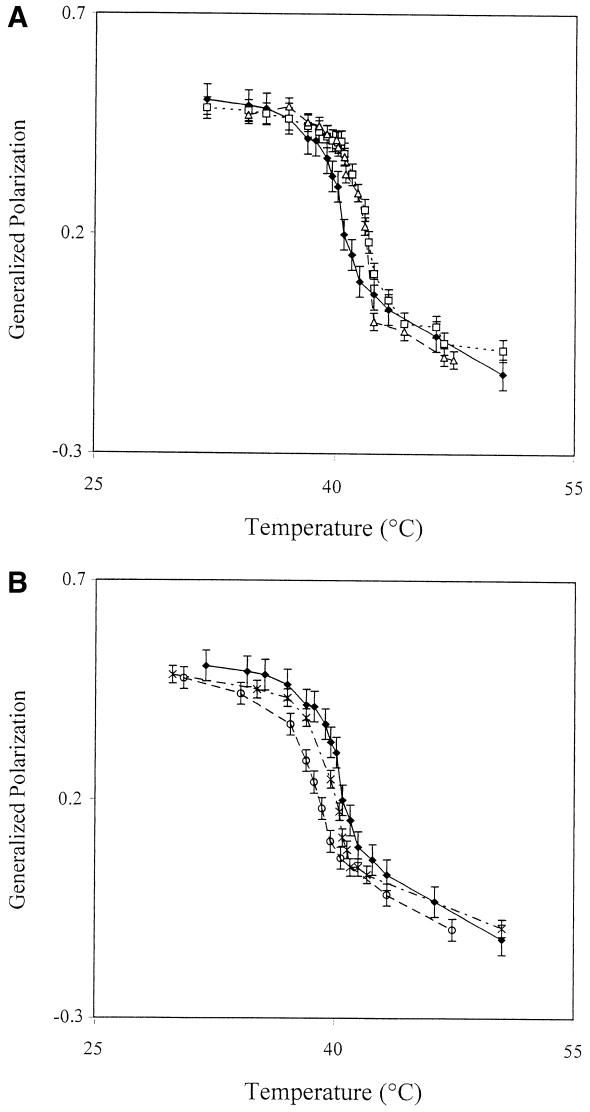

Fig. 2. Effect of *N*-acylethanolamines (NAEs) on Laurdan generalized polarization (GP) measured in DPPC LUVs as a function of temperature. Samples were suspended in 10 mM Hepes, 0.12 M NaCl, 5 mM KCl, and 0.1 mM EDTA buffer (pH 7.4). GP was calculated from Laurdan emission intensities at 440 nm and 490 nm as described in Materials and Methods (λex = 340 nm). A: Diamond, DPPC LUVs; square, *N*-palmitoylethanolamine (NPEA)-DPPC LUVs; triangle, *N*-stearoylethanolamine (NSEA)-DPPC LUVs. B: Triangle, DPPC LUVs; asterisk, NLEA-DPPC LUVs; circle, *N*-oleoylethanolamine (NOEA)-DPPC LUVs.

For a characterization of NAEs-DPPC ($R = 0.1$) interaction, the thermotropic behavior of Laurdan GP (calculated on emission spectra obtained by λex 340 nm), was measured (**Fig. 2A**, **B**). Previous studies demonstrated that DPPC LUVs and multilamellar vesicles (MLVs) have nearly identical phase behavior, with similar pretransition and a main transition (Tm) temperatures (39, 40). The gel-to-liquid-crystalline phase transition of DPPC LUVs is known to be highly cooperative (28 and references cited therein). Laurdan GP values (Fig. 2) show a large decrease at the main phase transition of DPPC LUV (Tm), while it is very hard to assess the presence of the pretransition by the small slope changes shown by GP curves although occurring at a temperature (~36.5°C), which is similar to previously reported data (39). For this reason, only the gel-to-liquid-crystalline phase transition will be discussed in all samples. As reported in **Table 1**, NOEA (C18:1) with a double bond in its acyl chain decreases the DPPC Tm (from 41°C to 39.4°C). In contrast, the other NAEs increase or decrease the lipid Tm with a pattern dependant on the length of their saturated acyl chains. The NAEs tested do not affect significantly the width of the gel-to-liquid-crystalline phase transition (Fig. 2), suggesting no lateral phase separation in lipid domains with different lipid compositions within the bilayer. However, the possible formation of small-scale clusters enriched with specific constituents cannot be excluded. Only NOEA slightly broadens the Tm range, suggesting the presence of domains of different lipid composition. Below and above the main lipid phase transition, Laurdan GP values are not largely modified, compared with pure DPPC, by the presence of NCEA (not shown), NPEA, and NSEA ($R = 0.1$ for all samples) (Fig. 2A). On the contrary,

TABLE 1. Effect of *N*-acylethanolamines on gel-to-liquid-crystalline phase transition temperature

Sample	Transition Temperature
DPPC	41.0°C
+NCEA	40.7°C
+NLEA	40.2°C
+NPEA	41.9°C
+NSEA	41.9°C
+NOEA	39.4°C

NCEA, *N*-caprinoylethanolamine; NOEA, *N*-oleoylethanolamine; NPEA, *N*-palmitoylethanolamine; NSEA, *N*-stearoylethanolamine. Effect of *N*-acylethanolamines (NAEs) on gel-to-liquid-crystalline phase transition temperature (Tm), measured by 2-dimethylamino-(6-lauroyl)-naphthalene (Laurdan) generalized polarization (GP) on dipalmitoylphosphatidylcholine (DPPC) large unilamellar vesicles (LUVs). DPPC was 0.3 mM, and the probe-lipid molar ratio was 1:1,000. NAE-DPPC molar ratio = 0.1. Results are presented as means. The SD was always ± 0.2.

NOEA-DPPC LUVs ($R = 0.1$) show lower GP values compared with DPPC at almost each temperature tested (Fig. 2B). This effect is more evident below Tm. A similar but less evident decrease is shown also by NLEA containing LUVs ($R = 0.1$) (Fig. 2B).

Effects of NAEs on PLA_2 activity

Previous studies demonstrated an enhanced PLA_2 activity at the PL gel-to-liquid-crystalline phase transition, where the lipid packing shows maximum heterogeneity (41). Moreover, the possible use of DPPC liposomes as NAEs delivery systems implicates their use at physiological temperatures. For these reasons, activity studies were performed at the temperature of 38.7°C, below the DPPC Tm (in LUV 41°C).

At this temperature, all samples tested ($R = 0.1$) are in the gel phase (Fig. 2), as confirmed by X-ray data (see the following section). In the case of NOEA ($R = 0.1$), the temperature 38.7°C may well be in the range of phase transition.

Normalized Laurdan emission spectra (**Fig. 3**) indicate that, at 38.7°C, NAEs ($R = 0.1$) modify the bilayer polarity at the glycerol level, in a manner dependent on the chain length and unsaturation. In fact, the spectrum is not significantly affected by NCEA (not shown); instead, it is enlarged and increased in intensity at longer wavelengths by NLEA and NOEA, (Fig. 3B) while it is narrowed and decreased in the red region (around 490 nm) by NPEA and NSEA (Fig. 3A). GP values were calculated from these spectra and are shown in **Table 2**, upper panel. It is evident that NLEA and, to a larger extent, NOEA, induce a decrease of GP values (Table 2, upper panel). These results indicate an increased polarity in these samples. On the contrary, NPEA and NSEA have an opposite effect on the polarity of the probe microenvironment, as indicated by the increased values of GP. Almost no changes are induced by NCEA on Laurdan GP.

Table 2 also reports GP values calculated from spectra recorded on the same samples after incubation with 0.5 μM PLA_2 in the absence of Ca^{2+}. No significant GP changes were measured after enzyme incubation. These results indicate that before Ca^{2+} addition, the enzyme does not significantly perturb the Laurdan microenvironment, either in the absence or in the presence of NAEs ($R = 0.1$).

The fluorescence features of Laurdan and Prodan were used to study PLA_2 activity. Laurdan and Prodan are similar probes that differ only in the length of their hydrophobic tail (12 C and 3 C atoms, respectively). The use of

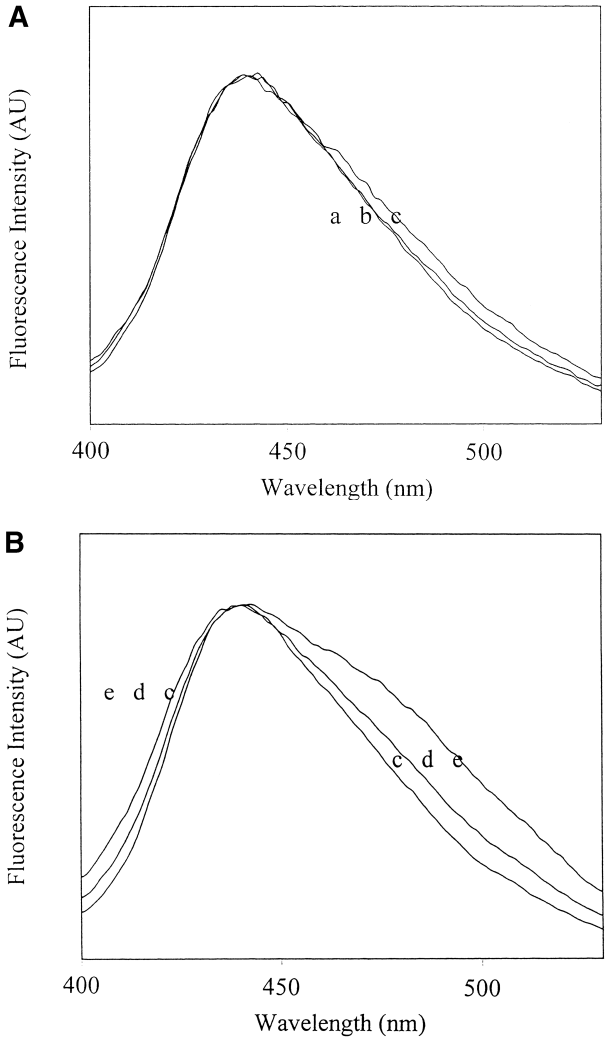

Fig. 3. Normalized steady-state fluorescence emission spectra of Laurdan in DPPC LUVs: effect of NAEs. Samples were suspended in 10 mM Hepes, 0.12 M NaCl, 5 mM KCl, and 0.1 mM EDTA buffer (pH 7.4). Spectra were recorded at λex = 340 nm. T = 38.7°C. A: curves: a, NPEA-DPPC LUVs; b, NSEA-DPPC LUVs; c, DPPC LUVs. B: Curves: c, DPPC LUVs; d, NLEA-DPPC LUVs; e, NOEA-DPPC LUVs.

TABLE 2. Laurdan GP values in liposomes containing NAEs

	A	B
$R = 0.1$		
DPPC	0.425 ± 0.021	0.432 ± 0.017
+ NCEA	0.406 ± 0.007	0.401 ± 0.008
+ NLEA	0.370 ± 0.018[a]	0.369 ± 0.003[a]
+ NPEA	0.458 ± 0.010[b]	0.458 ± 0.006[c]
+ NSEA	0.455 ± 0.020[c]	0.455 ± 0.026[c]
+ NOEA	0.234 ± 0.026[a]	0.219 ± 0.027[a]
$R = 0.01$		
DPPC	0.425 ± 0.021	0.432 ± 0.017
+ NCEA	0.420 ± 0.010	0.419 ± 0.014
+ NLEA	0.414 ± 0.009	0.423 ± 0.007
+ NPEA	0.438 ± 0.011	0.448 ± 0.005
+ NSEA	0.431 ± 0.007	0.430 ± 0.005
+ NOEA	0.381 ± 0.006[d]	0.399 ± 0.013[c]

GP values for Laurdan embedded in DPPC LUVs in the presence and in the absence of NAEs. T = 38.7°C. For other experimental conditions, see Table 1. Results are means ± SD. Significance was tested by Student's *t*-test. A: In the absence of phospholipase A_2 (PLA_2). B: In the presence of PLA_2. R = NAE-DPPC molar ratio.

[a] $P < 0.001$ compared with the control evaluated in the same conditions.

[b] $P < 0.005$ compared with the control evaluated in the same conditions.

[c] $P < 0.05$ compared with the control evaluated in the same conditions.

[d] $P < 0.01$ compared with the control evaluated in the same conditions.

these probes to study the physico-chemical changes occurring in the bilayer during the PLA_2-induced hydrolysis was introduced and characterized in previous works (21, 24, 26). In the presence of zwitterionic PL vesicles, PLA_2 activity is characterized by a latency period (identified as τ or lag time) of slow rate, followed by an abrupt increase of the hydrolytic rate. The length of lag time is dependent on various factors, such as structure, composition, and bilayer dynamics. Moreover, the abrupt increase of hydrolysis rate is believed to be dependent on the formation of threshold concentrations of the reaction products. Laurdan and Prodan spectral changes in DPPC bilayers were correlated with the presence of the hydrolytic products (21, 24, 26) [palmitic acid and lysophosphatidylcholine (Lyso-PC)].

The contemporary use of these probes is particularly useful because they locate in two different environments within the bilayer, since Prodan is located in the region of polar headgroups, while Laurdan is at the hydrophilic-hydrophobic interface (34) (at the glycerol backbone).

Laurdan is tightly anchored by its long lauric-acid tail to a single site in the bilayer (42) both in gel and liquid-crystalline phases, while Prodan molecules were suggested to be distributed in the bilayer among different environments, depending on the physical state of the membrane (43).

The time course of PLA_2 hydrolytic activity on DPPC LUVs was derived by measuring the ratio between the intensities at 490 nm and 440 nm (R/B) on both Laurdan and Prodan fluorescence emission spectra (**Fig. 4**). In our experimental conditions, PLA_2 activity toward DPPC LUVs presents a lag time of 740 ± 102 s when it is measured using the Laurdan R/B. A similar lag time was obtained by measuring the time course of Prodan R/B (Fig. 4) (800 ± 105 s).

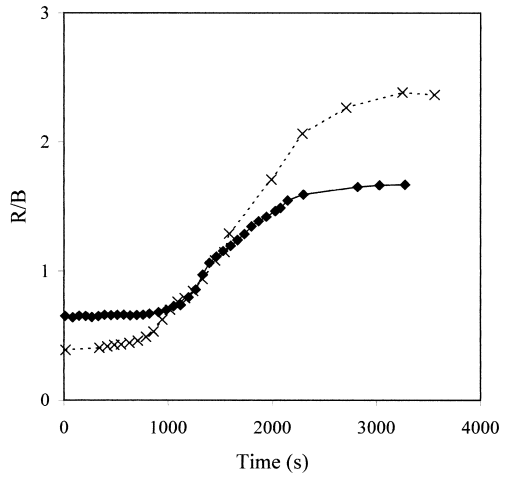

Fig. 4. Time courses of 6-propionyl-2-(dimethylamino)-naphthalene (Prodan) and Laurdan fluorescence during DPPC LUV hydrolysis. The reaction was triggered by the addition of 5 mM $CaCl_2$ to the sample containing DPPC and phospholipase A_2 (PLA_2). T = 38.7°C. The intensities at 490 nm and 440 nm were measured for both probes on steady-state fluorescence emission spectra (λex = 359 nm for Prodan and λex = 340 nm for Laurdan). A ratio of 490 nm to 440 nm (R-B) is reported for both Prodan (triangle) and Laurdan (x).

Previous data (26), performed by Asp-49 PLA_2 from *Agkistrodom piscivorus piscivorus* venom on DPPC LUVs, demonstrated that the abrupt increase of Prodan R-B ratio, which occurs during the hydrolysis, is coincident with the raise of the enzymatic activity at time τ. This PLA_2 activation is due to an increased enzyme-interface interaction at this time. In that work (26), the lag time measured by Laurdan fluorescence was not coincident with that obtained by Prodan. This different behavior was explained by the higher sensitivity of Prodan emission spectra to the presence of Lyso-PC, which disrupts the bilayer in the region of PL headgroups (26). On the contrary, it was shown that Laurdan fluorescence is less useful for probing PLA_2 membrane degradation occurring during the hydrolysis because it is more sensitive to the stabilizing effect of fatty acids than to Lyso-PC (26) accumulation. However, the comparison with other data performed on DPPC LUVs by the same group (21) suggests that, in our experimental conditions (pH 7.4 and 5 mM Ca^{2+}), the fatty acids formed during DPPC hydrolysis are continuously extracted from the bilayer.

It was in fact suggested that Ca^{2+} concentrations >10 μM decrease the amount of charged palmitic acid (pK = 7.5–8.5 in the bilayer) in the membrane (21). Therefore, it is hypothesized that, in our conditions, both Prodan and Laurdan give similar results because the fatty acid content in the membrane is lower than Lyso-PC content. In fact, it was demonstrated that increasing concentrations of Lyso-PC affect the fluorescence of both probes in a similar way (26). In our samples, similar lag times were obtained either by Laurdan R-B ratio or GP calculated by the same emission wavelengths (unpublished observations). For this reason, the following experiments will show lag times measured by using Laurdan GP data. **Figure 5A** and **B** report the time courses of vesicle hydrolysis in DPPC LUVs in the presence and in the absence of the desired NAE. It is evident that NAEs (R = 0.1) modify PLA_2 lag times (correspondent to the latency period) in a way that is dependent on the acyl chain length and unsaturation. Lag times (**Table 3**, upper panel) are largely decreased by NLEA and NPEA (−38.8% and −44.7% compared with pure DPPC, respectively), are almost unchanged by NCEA (not shown), and are only slightly modified by NSEA and NOEA (−16.5% and +14.1%, respectively). Control experiments revealed that NAEs, which are added as exogenous molecules to DPPC LUVs, modify the time courses of vesicle hydrolysis in a way similar to that reported in Fig. 5 (not shown).

To evaluate the effect of lower concentrations of NAEs on PLA_2 activity, further experiments were performed using an NAE-DPPC (R = 0.01). At this NAEs concentration, Laurdan GP values are significantly modified only by NOEA (Table 2, lower panel). Lag times (Table 3, lower panel) are decreased by NLEA and, to a minor extent, by NPEA (−26% and −14%, respectively), are unmodified by NCEA, and are increased by NSAE and NOEA (+23% and +24%, respectively).

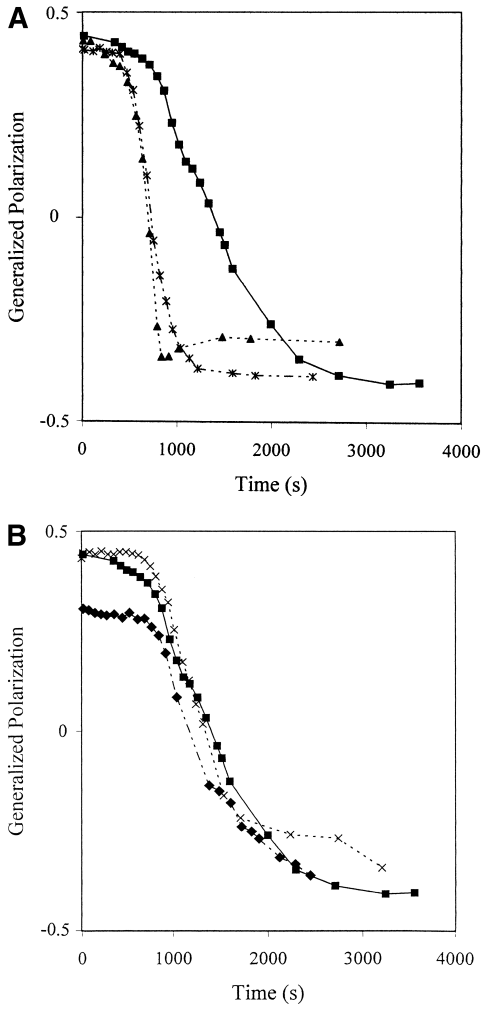

Fig. 5. Time courses of Laurdan fluorescence during hydrolysis of DPPC LUVs: effect of NAEs. Reaction conditions were identical to those in Fig. 4. Laurdan fluorescence is expressed as GP, which was calculated from emission intensities at 440 nm and 490 nm, as described in Materials and Methods (λex = 340 nm). T = 38.7°C. A: Square, DPPC LUVs; asterisk, NLEA-DPPC LUVs; triangle, NPEA-DPPC LUVs. B: Square, DPPC LUVs; x, NSEA-DPPC LUVs; diamond, NOEA-DPPC LUVs.

Prodan steady-state fluorescence

The fluorescent probe was used to elucidate the possible different modulation of PL water content and dynamics by NSEA and NPEA. As is Laurdan, Prodan fluorescence is sensitive to the dipolar relaxation phenomenon (35). However, in contrast to Laurdan, Prodan's shorter acyl residue locates the probe near the bilayer surface and affects its affinity for the membrane and different lipid phases (35). It is known that Prodan partitioning in the bilayer is dependent on the membrane order degree (35) since, for its short hydrophobic chain, it is squeezed out from a well-packed lipid phase to the bulk water. Similarly to Laurdan, this probe is sensitive to the content and dynamic of water molecules in the bilayer (35). Moreover, the recently introduced Prodan 3wGP parameter is similar to Laurdan GP and is sensitive to PL phase state. In particular, Prodan 3wGP was demonstrated to detect structural changes involving the PL headgroup region (35). Prodan spectra present a quite relevant intensity in the red wavelengths region, with the presence of an additional band at ~520 nm. This band is due to Prodan molecules in the aqueous phase (35). According to Krasnowska et al. (35), the GP was calculated measuring the emission intensity at three wavelengths (3wGP) chosen to maximize the separation of the contributions from the different Prodan environments. The 3wGP method allows the measurement of the probe Cp between the bilayer and water (35). Results are reported in **Table 4**. Both the blue shift of the Prodan emission spectrum (data not shown) and the 3wGP increase (from 0.309 ± 0.025 in DPPC to 0.405 ± 0.018 in NPEA/DPPC, and 0.374 ± 0.022 in NSEA/DPPC) indicate that NPEA and NSEA cause a lower bilayer polarity in the microenvironment sensed by Prodan. Moreover, the NAEs-induced decrease of Cp indicates an increased exposure of Prodan to bulk water (Table 4). All these effects are more evident for NPEA.

TABLE 3. PLA_2 lag time measurements

	Lag Time (s)	% Change
$R = 0.1$		
DPPC	740 ± 102	0
+ NCEA	785 ± 39	+ 6.1
+ NLEA	453 ± 133[a]	−38.8
+ NPEA	409 ± 118[a]	44.7
+ NSEA	618 ± 37[b]	16.5
+ NOEA	844 ± 114	+14.1
$R = 0.01$		
DPPC	740 ± 102	0
+ NCEA	760 ± 105	+ 3.0
+ NLEA	550 ± 9[b]	−26.0
+ NPEA	633 ± 173	−14.0
+ NSEA	913 ± 35[b]	+23.0
+ NOEA	888 ± 136	+20.0

Pancreatic PLA_2 activity was measured by Laurdan GP on DPPC LUVs, in the absence and in the presence of saturated and monounsaturated NAEs. Reaction mixture contained 0.5 μM PLA_2 and 0.3 mM DPPC. T = 38.7°C. Results are means ± SD. Significance was tested by Student's *t*-test. R = NAE-DPPC molar ratio.

[a] $P < 0.010$.

[b] $P < 0.050$.

X-ray diffraction data

X-ray diffraction data were acquired in DPPC MLVs prepared in the absence or in the presence of NAEs (NAE-DPPC molar ratio, $R = 0.1$).

TABLE 4. 6-propionyl-2-(dimethylamino)-naphthalene three-wavelengths GP and partition coefficients of the probe between phospholipids (PLs) and buffer

Sample	3wGP	Cp × 10^4
DPPC	0.309 ± 0.025	17.8 ± 1.1
+NPEA	0.405 ± 0.018[a]	12.4 ± 0.3[b]
+NSEA	0.374 ± 0.022[a]	14.2 ± 0.5[b]

Cp, partition coefficients; Prodan, 6-propionyl-2-(dimethylamino)-naphthalene; 3wGP, three-wavelengths GP; PL, phospholipids. T = 38.7°C. Results are presented as means ± SD. Significance was tested by Student's *t*-test.

[a] $P < 0.001$.

[b] $P < 0.05$.

Three different lamellar phases, namely the L_β', P_β', and L_α phases, are observed as a function of temperature for the fully hydrated DPPC MLV system. The phase transitions from L_β' to P_β' and from P_β' to L_α are usually indicated as pretransition and main transition, respectively. These lamellar structures are characterized by a distorted pseudo-hexagonal, hexagonal, and liquid-like arrangement of the hydrocarbon chains inside the layer, respectively (44, 45). Moreover, in the P_β' phase, the lipid bilayers are distorted by a periodic ripple so that the structure presents a 2-dimensional lattice (46).

Measurements were performed at the fixed temperature 38.7°C. The main purpose was to determine if the presence of NAEs can induce the transition from the lamellar to a different lipid phase. Moreover, X-ray experiments were used to assess the possible presence of phase coexistence, even if the method can underline only the large multiphase domains. The low-angle (**Fig. 6**) and high-angle (**Fig. 7**) diffraction patterns have been considered separately. The low-angle diffraction patterns observed in all samples (Fig. 6) are characterized by three and/or four sharp peaks; their spacing clearly indicates a one-dimensional lamellar lattice (1:2:3:4, etc.). Therefore, information about the interlamellar repeat distances can be derived. However, in our experimental conditions (excess buffer), it is not possible to separate the contributions of the lipid and water layers to the measured periodicity (47). The calculated unit cell dimensions (**Table 5**) are: 71.7 ± 0.5 Å for DPPC, 76.8 ± 0.5 Å for NLEA-DPPC, 72.5 ± 0.5 Å for NSEA-DPPC, and 70.1 ± 0.5 Å for NPEA-DPPC. Note that the unit cell corresponds to the distance between the mid-plane of two opposing lipid bilayers. The absence of other peaks in the spectra gives clear evidence that each sample is characterized by a single pure phase.

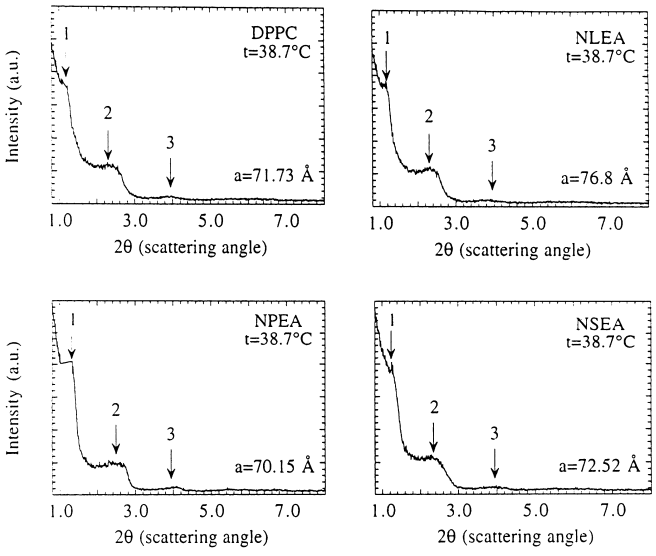

Fig. 6. X-ray low-angle diffraction profiles obtained for fully hydrated DPPC multilamellar vesicles (MLVs) prepared in the absence and in the presence of NAEs. NAE-DPPC molar ratio was $R = 0.1$. Data were acquired at 38.7°C . The Bragg peaks are indexed according to the Miller indexes *h00* of the reflection. The corresponding unit cells are indicated.

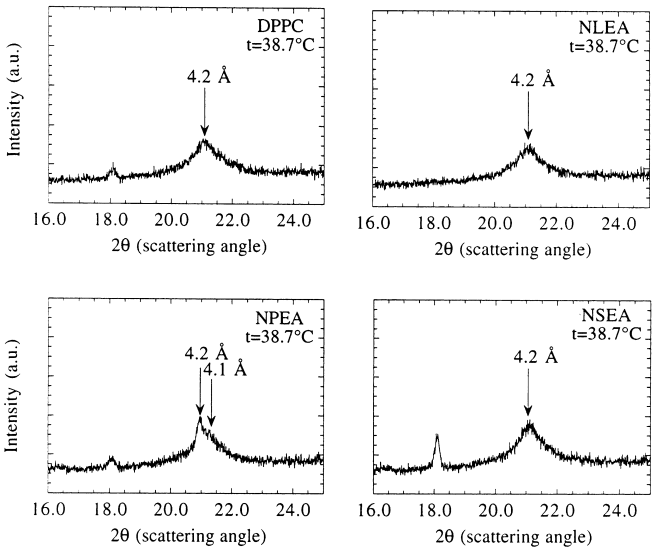

Fig. 7. X-ray high-angle diffraction profiles obtained for fully hydrated DPPC MLVs prepared in the absence and in the presence of NAEs. NAE-DPPC molar ratio was $R = 0.1$. Data were acquired at 38.7°C . The peak positions are reported, indicating the corresponding interchain distances, as calculated by using the Bragg law. The peak centered at $2\theta = 18°$ is due to the sample-holder mylar windows.

The high-angle region gives information on the PL hydrocarbon tails: in particular, two peaks characterize the L_β' phase, while a single peak is observed in the P_β' phase. The high-angle diffraction data reported in Fig. 7 demonstrate that DPPC, NLEA-DPPC, and NSEA-DPPC samples are in the P_β' phase, while NPEA-DPPC is in the L_β' phase. Either the reflections centered at about 4.2 Å (DPPC, NLEA-DPPC, and NSEA-DPPC) or those centered at 4.2 Å and 4.1 Å (NPEA-DPPC) (Table 5) give the reason why there are no changes with respect to the typical spectra observed in the same phases for pure DPPC, close to the pretransition temperature.

DISCUSSION

PLA_2 is an interfacially activated soluble enzyme whose activity occurs in two distinct steps: *1*) the enzyme binds to the vesicle surface, becoming activated; *2*) the activated

TABLE 5. X-ray diffraction data in liposomes containing NAEs

	Low-Angle	High-Angle	
Compounds	*a* (Å)	d (Å)	d (Å)
DPPC	71.7	4.2	—
NLEA	76.8	4.2	—
NPEA	70.1	4.2	4.1
NSEA	72.5	4.2	—

X-ray diffraction data recorded in fully hydrated multilamellar vesicles samples at 38.7°C. The interlamellar repeat distances *a* (Å) and the interchain distances d (Å) are reported. SD for low- and high-angle data was always 0.5 and 0.03, respectively.

enzyme binds a molecule of substrate PL at the catalytic site, generating the hydrolysis products. Secreted PLA_2 requires Ca^{2+} as cofactor.

Although the molecular mechanism of this interfacial activation is not clarified, it appears that PLA_2 activity is affected by bilayer physical properties. In fact, exogenous molecules or other factors that modify the physical properties of the bilayer are known to affect the enzymatic activity. For example, it was shown that several lipophilic compounds reduce the rate of lipid hydrolysis by affecting the bilayer physical properties in a way that promotes desorption of bound enzymes (48). Moreover, factors that allow an easier access of the enzyme to substrate shift the reaction equilibrium toward the products. These factors can be various; for example, the high curvature of the bilayer or the presence of cone-shaped lipids, such as cardiolipin or DAG (49 and references cited therein).

In general, the PLA_2 hydrolitic activity is significantly affected by the presence of lipid lateral segregation into domains and by other bilayer defects, which can be in the form of holes in the bilayer (50, 51), or line defects occurring in bilayers undergoing density fluctuations near the main-phase Tm (41). In fact, the increase of PLA_2 activity near the lipid Tm was related to the contemporary increase of the heterogeneous lateral bilayer structure (41) due to thermal density fluctuations. Since NAEs modify physico-chemical bilayer properties, the effect of these hydrophobic molecules on the PLA_2 activity was examined.

Pig pancreas PLA_2 (classified as type I of the enzymatic family) (52) was chosen for this study because it is recognized to represent a good model for in vitro studies of phospholipase activity (53, 54). Moreover, studies on this protein are interesting because the presence of type I PLA_2 proteins was demonstrated in various tissues, including kidney, small intestine, spleen, lung, and stomach (55). A pancreatic type I PLA_2 was recently identified in the human epidermis (56). Moreover, the presence of a PLA_2, which is revealed by immunostaining with antibodies raised against the porcine pancreatic enzyme, was detected in the acrosomal region of human spermatozoa (57).

Each sample tested ($R = 0.1$) did not show evident phase separation within the bilayer, as evidenced by X-ray diffraction experiments and Laurdan GP thermotropic behavior. Only NOEA shows a slightly larger width of the main transition, which is shifted to low temperatures. This width could reflect a lipid bilayer heterogenity, likely due to the presence of unsaturation, which decreases the acyl chain packing. Lipid Tm changes, measured by Laurdan, indicating that saturated NAEs (characterized by a long acyl chain, an amide linkage, and the free hydroxyl group of ethanolamine) affect DPPC Tm following a similar pattern to alcohols. In fact, it is known that short-chain n-alkanols decrease the temperature of the PL main transition, while molecules with a carbon chain longer than 10–12 carbon atoms (cut-off length) increase it (58, 59). Laurdan data suggest that, at 38.7°C, NLEA- and NOEA-containing samples will be closer to lipid main-phase transition if compared with pure DPPC LUVs and LUVs containing longer NAEs. It is known that PLA_2 activity toward pure DPPC LUVs displays a maximum (corresponding to a minimum of lag time) at the gel-to-fluid phase Tm. This effect was related to the thermal density fluctuations inducing the dynamic formation of small-scale gel-fluid lipid domains, and hence microheterogeneity (28, 41).

An increasing degree of microheterogeneity is expected for a bilayer that is approaching the Tm. Due to the effect of NLEA and NOEA on the gel-to-liquid-crystalline temperature transition, a NLEA- and NOEA-induced increase of PLA_2 activity was expected, with respect to the control, as a consequence of an increased degree of lateral heterogeneity. An opposite effect was expected for NPEA and NSEA. As predicted, the presence of NLEA increases the PLA_2 activity (i.e., it induces a lag time decrease), while NCEA does not modify it. However, the effect of the other NAEs on lag time was unexpected. The slight inhibitory effect of NOEA (measured for both NOEA concentrations used) could be related to the large decrease of lipid chain packing caused by the presence of unsaturation at Carbon 9 and suggested by the low Laurdan GP values measured at temperatures below those of the main lipid phase transition. This membrane disorganization is close to the membrane interfacial region, and it could avoid the optimal enzyme-lipid interaction. In fact, in pancreatic enzymes, this interaction requires that flexible regions in the free enzyme, such as the N-terminus and the surface loop, become more ordered in the complexed form (60). This effect could be prevented by the membrane disorganization induced by NOEA. Another possibility is that PLA_2 could dig into the membrane, while a superficial localization is necessary for a good hydrolytic activity (60).

In order to explain the results obtained with saturated NAEs, we propose that the cause of NAEs' effect on PLA_2 activity can be their localization in the bilayer, which could be determined by the particular structural properties of these molecules; i.e., the presence of two groups that can form hydrogen bonds (hydroxyl and amide groups) and the long acyl chain. We hypothesize that the chain length can affect the partition coefficient of the NAE within the membrane and/or the localization along the normal to the bilayer plane. The reduced perturbation of DPPC bilayer by NCEA could be a consequence of a low-partition coefficient due to relatively low energy gain by van der Waals interactions with lipid acyl chains, which can be overlaid by the hydrogen bond formation with solvent molecules and/or PL headgroups. The additional two carbons of the NLEA acyl chain could be critical for its incorporation within the bilayer. However, the DPPC Tm lowering suggests an NLEA-induced bilayer disorganization due to an improper fit of the hydrocarbon chain into the membrane matrix. This effect could create voids in the hydrocarbon core, as previously suggested for 1-alkanols with similar carbon chain length (61). The NPEA- and NSEA-induced increase of DPPC Tm could be explained, assuming that these molecules

enhance the lipid-lipid interactions and participate in them, similarly to alcohols with the same number of carbon atoms (61). However, in spite of NPEA's and NSEA's similar action on lipid Tm and on the polarity of the Laurdan microenvironment, their PLA_2 activity modulation is different. We suggest that NLEA and NPEA can be linked to PL headgroups by two hydrogen bonds: the nitrogen atom of the amide could interact with the carbonyl group of the *sn*-2 acyl chain, while the hydroxyl group of NAE could be hydrogen bonded with the phosphate group. The long, unfolded chain of NSEA (18:0) could avoid a proper localization of the amide and hydroxyl groups in the bilayer by shifting them in a too-high position to form hydrogen bonds with acceptor groups in DPPC. The model proposed could explain the increased activity by NLEA and NPEA, which can introduce a surface heterogeneity by creating a large void in the headgroup region and permitting a PLA_2 greater access to the *sn*-2 bonds of the substrate. This hypothesis is in line with the behavior suggested by Henshaw et al. (21) for protonated palmitic acid, which forms hydrogen bonds with the PL phosphate group, descending deeper in the bilayer than the ionized form. On the contrary, the low effect of NSEA on PLA_2 activity could be due to its higher position in the bilayer. In this case, the slight decrease of lag time could be due to a decreased formation of voids in the headgroup region. However, results obtained with NSEA/DPPC $R = 0.01$ vesicles could suggest another possible mechanism for NSEA action. In fact, Laurdan GP temperature dependence curves (Fig. 2) cannot exclude the possible formation of small-scale clusters of different lipid compositions for each sample studied. The presence of such clusters could affect bilayer heterogeneity, which appears to be important to promoting the Ca^{2+}-dependent Step 2 (21 and references cited therein). The possible presence of these clusters could be supported by results obtained with the lower NAE concentration ($R = 0.01$). In fact, the opposite effect shown by the two concentrations of NSEA ($R = 0.1$ and $R = 0.01$) on PLA_2 activity could be explained by hypothesizing the contemporary action of two different effects. In the case of $R = 0.1$, the activating effect, due to the heterogeneity introduced in the bilayer by these small clusters, could counteract the inhibiting action due to the NSEA-induced enhanced lipid-lipid interaction. In the case of $R = 0.01$, the cluster formation could be negligible, and the inhibiting action of NSEA could prevail. In fact, it is known that an increased cohesion of the lipid bilayer is detrimental to the lytic action of the enzyme (49). The hypothesis of different NPEA and NSEA interactions with DPPC headgroups is supported by Prodan results, which indicate an NAEs-induced reduced polarity in the probe microenvironment of these samples. This effect is likely due to an increased PL ordering, which is suggested by 3wGP values (in the order NPEA>>NSEA>DPPC) and by the Prodan repartition Cp. Cp values indicate that probe exposure to bulk water increases in the order DPPC<NSEA<NPEA. This ordering effect is in line with the hypothesis of different NAE-PC interactions for NPEA and NSEA, with the possible formation of strong hydrogen bonds NPEA-PC and of weaker interactions NSEA-PC at the headgroup level. Also, X-ray data confirm the hypothesis of different NAE interactions at the lipid polar headgroups. In fact, at 38.7°C, NPEA-containing DPPC MLV samples are in L_β' phase, while NSEA-containing DPPC liposomes are in P_β', indicating an NPEA-induced shift of L_β'- P_β' lipid transition (pretransition) to higher temperatures. These results confirm the hypothesis of strong interactions affecting the pretransition in the lipid-polar headgroup region. Furthermore, the presence of the P_β' phase in NLEA-DPPC samples is not surprising, because, as previously discussed, NLEA's shorter acyl chain, compared with the palmitoyl chains of the phosphatidylcholine, likely induces bilayer core disorganization and, as a consequence, a decrease of phase transitions temperatures. Moreover, the calculated cell dimensions indicate that the DPPC interlamellar repeat distance is largely increased by NLEA, while only a small effect is induced by NSEA. NLEA-induced results could be indicative of a phase change (i.e., a change in the lipid molecular organization) or an increase of the water thickness between the lipid bilayers. Since the high-angle profile of DPPC-NLEA excludes a phase change, it is deduced that the water thickness is increased, in agreement with a possible increased hydration of PL headgroups. A possible increase of PL headgroups hydration, without phase change, can be deduced also by data reported for DPPC-NPEA. In fact, the calculated cell dimensions for the L_β' phase in this sample are significantly different from the values usually reported for pure DPPC in the same phase (about 64 Å) (47). These measurements suggested an NPEA- and NLEA-induced increase of interlamellar water layer likely correlated with an increased hydration of PC headgroups, in agreement with the hypothesis of the presence of void spaces in this bilayer region.

The possible different localization of NAEs in the bilayer could affect the PLA_2 adsorption at the membrane surface, also in the absence of Ca^{2+}. However, data reported in Table 2 indicate that membrane physico-chemical properties probed by Laurdan are unaffected by the presence of the enzyme in the absence of the cation. These results could suggest that NAEs modulate the enzymatic activity without increasing the number of adsorbed enzyme molecules in Step 1. Recent works proposed that membrane surface defects could modify the PLA_2 enzymatic activity by altering the equilibrium of Ca^{2+}-dependent Step 2 (26) and by allowing the PLA_2 active site greater access to the *sn*-2 bond of phosphatidylcholine (21). Moreover, an action at Step 2 was suggested for unionized palmitic acid (21). The comparison with our data could indicate that NAEs affect the enzymatic activity at Step 2. However, it is likely to be excluded that NAEs could increase the ability of the substrate molecule to leave the plane of the bilayer, which is a possible mechanism of Step 2 (21, 26). This hypothesis is suggested because the PLA_2 activity is almost unmodified by the presence of NOEA, although this unsaturated molecule largely disorganizes the membrane structural matrix in

the gel phase, suggesting an increased possibility of lipid substrate leaving the membrane.

Conclusions

The NAEs' lipophilicity provides opportunity to examine the interaction of these molecules with lipids, which could have important pharmacological actions. Fluorescence and X-ray techniques help to understand NAE's interaction with a PC liposome, providing information about structural and physico-chemical changes induced by these molecules on the bilayer. The NAE concentrations used in this work are not normally present in membranes (2), although the NAE-DPPC molar ratio $R = 0.01$ could be reached in some conditions. In fact, in ischemic canine heart, NAEs can be accumulated to a level of 400–500 nmol/g tissue (2), which corresponds, assuming 20 μmol lipid phosphorous/g tissue (2), to a NAE-PL molar ratio of 0.020:0.025. Moreover, the possible preferential NAE localization in specific membrane domains with different lipid compositions could give rise to microenvironments with different structural and physico-chemical features, as suggested by our present data and a previous work, which demonstrated the formation of a cubic phase when NAEs interact with egg phosphatidylethanolamine (16). For this reason, data on NAE's effects on PLA_2 activity could support the hypothesis that some physiological functions of NAEs could be performed through the modulation of structural and physico-chemical membrane features (1, 16, 17).

Moreover, our results could be useful for projecting a proper system for delivering pharmacologically active NAEs to tissues. In fact, small-sized liposomes with a rigid bilayer are considered suitable carrier systems for target drug delivery to tumors and inflammatory foci (62), and recent studies suggested that their use for a possible targeted transport to pathological tissues (e.g., in inflammation) could be linked to their degradation by membrane active and destabilization enzymes, such as PLA_2 (63), whose activity is often locally increased in such tissues (64, 65).

This work was supported by Ministero Italiano dell'Università e della Ricerca Scientifica (MURST) to G.Z. and Komitet Badañ Naukowych grant 6905A06220 to M.W.

REFERENCES

1. Schmid, H. H. O., P. C. Schmid, and V. Natarajan. 1990. *N*-acylated glycerophospholipids and their derivatives. *Prog. Lipid Res.* **29:** 1–43.
2. Hansen, H. S., B. Moesgaard, H. H. Hansen, and G. Petersen. 2000. *N*-Acylethanolamines and precursor phospholipids - relation to cell injury. *Chem. Phys. Lipids.* **108:** 135–150.
3. Giuffrida, A., and D. Piomelli. 1998. Isotope dilution GC/MS determination of anandamide and other fatty acylethanolamides in rat blood plasma. *FEBS Lett.* **422:** 373–376.
4. Zolese, G., G. Falcioni, E. Bertoli, R. Galeazzi, M. Wozniak, Z. Wypych, E. Gratton, and A. Ambrosini. 2000. Steady-state and time resolved fluorescence of albumins interacting with *N*-oleylethanolamine, a component of the endogenous *N*-acylethanolamines. *Proteins.* **40:** 39–48.
5. Giuffrida, A., F. Rodriguez de Fonseca, F. Nava, P. Loubet-Lescoulie, and D. Piomelli. 2000. Elevated circulating levels of anandamide after administration of the transport inhibitor, AM404. *Eur. J. Pharmacol.* **408:** 161–168.
6. Kondo, S., T. Sugiura, T. Kodaka, N. Kudo, K. Waku, and A. Tokumura. 1998. Accumulation of various *N*-acylethanolamines including *N*-arachidonoylethanolamine (anandamide) in cadmium chloride-administered rat testis. *Arch. Biochem. Biophys.* **354:** 303–310.
7. De Petrocellis, L., D. Melck, T. Bisogno, and V. Di Marzo. 2000. Endocannabinoids and fatty acid amides in cancer, inflammation and related disorders. *Chem. Phys. Lipids.* **108:** 191–209.
8. Berdyshev, E. V., P. C. Schmid, R. J. Krebsbach, C. J. Hillard, C. Huang, N. Chen, Z. Dong, and H. H. O. Schmid. 2001. Cannabinoid-receptor-independent cell signalling by *N*-acylethanolamines. *Biochem. J.* **360:** 67–75.
9. Mechoulam, R., E. Fride, and V. Di Marzo. 1998. Endocannabinoids. *Eur. J. Pharmacol.* **359:** 1–18.
10. Jonsson, K. O., S. Vandevoorde, D. M. Lambert, G. Tiger, and C. J. Fowler. 2001. Effects of homologues and analogues of palmitoylethanolamide upon the inactivation of the endocannabinoid anandamide. *Br. J. Pharmacol.* **133:** 1263–1275.
11. Calignano, A., G. La Rana, and D. Piomelli. 2001. Antinociceptive activity of the endogenous fatty acid amide, palmitylethanolamide. *Eur. J. Pharmacol.* **419:** 191–198.
12. Lambert, D. M., S. Vandevoorde, K. O. Jonsson, and C. J. Fowler. 2002. The palmitoylethanolamide family: a new class of anti-inflammatory agents? *Curr. Med. Chem.* **9:** 663–674.
13. Hansen, H. S., L. Lauritzen, B. Moesgaard, A. M. Strand, and H. H. Hansen. 1998. Formation of *N*-acyl-phosphatidylethanolamines and *N*-acylethanolmines. Proposed roles in Neurotoxicity. *Biochem. Pharmacol.* **55:** 719–725.
14. Schuel, H., E. Goldstein, R. Mechoulam, A. M. Zimmerman, and S. Zimmerman. 1994. Anandamide (arachidonylethanolamide), a brain cannabinoid receptor agonist, reduces sperm fertilizing capacity in sea urchins by inhibiting the acrosome reaction. *Proc. Natl. Acad. Sci. USA.* **91:** 7678–7682.
15. Sustin-Brown, S. L., and K. Chapman. 2002. Inhibition of Phospholipase Dα by *N*-acylethanolamines. *Plant Physiol.* **129:** 1892–1898.
16. Ambrosini, A., E. Bertoli, P. Mariani, F. Tanfani, M. Wozniak, and G. Zolese. 1993. *N*-acylethanolamines as membrane topological stress compromising agents. *Biochim. Biophys. Acta.* **1148:** 351–355.
17. Ambrosini, A., F. Tanfani, E. Bertoli, M. Wozniak, Z. Wypych, and G. Zolese. 1993. Effect of *N*-acylethanolamines with different acyl-chains on DPPC multilamellar liposomes. *Chem. Phys. Lipids.* **65:** 165–169.
18. Sprong, H., P. van der Sluijs, and G. van Meer. 2001. How proteins move lipids and lipids move proteins. *Nat. Rev. Mol. Cell Biol.* **2:** 504–513.
19. Hoop, B., and C. K. Peng. 2000. Fluctuations and fractal noise in biological membranes. *J. Membr. Biol.* **177:** 177–185.
20. Epand, R. M., and R. Kraayenhof. 1999. Fluorescent probes used to monitor membrane interfacial polarity. *Chem. Phys. Lipids.* **101:** 57–64.
21. Henshaw, J. B., C. A Olsen, A. R. Farnbach, K. H. Nielson, and J. D. Bell (1998) Definition of the specific roles of lysolecithin and palmitic acid in altering the susceptibility of dipalmitoylphosphatidylcholine bilayers to phospholipase A2. *Biochemistry.* **37:** 10709–10721.
22. Jain, M. K., M. H. Gelb, J. Rogers, and O. G. Berg. 1995. Kinetic bases for interfacial catalysis by Phospholipase A2. *Methods Enzymol.* **249:** 567–614.
23. Bell, J. D., and R. L. Biltonen. 1992. Molecular details of the activation of soluble phospholipase A2 on lipid bilayers. Comparison of computer simulations with experimental results. *J. Biol. Chem.* **267:** 11046–11056.
24. Bell, J. D., M. Burnside, J. A. Owen, M. L. Royall, and M. L. Baker. 1996. Relationships between bilayer structure and phospholipase A2 activity: interactions among temperature, diacylglycerol, lysolecithin, palmitic acid, and dipalmitoylphosphatidylcholine. *Biochemistry.* **35:** 4945–4955.
25. Vermehren, C., T. Kielber, I. Hylander, T. H. Callisen, and K. Jørgensen. 1998. Increase in phospholipase A2 activity towards lipopolymer-containing liposomes. *Biochim. Biophys. Acta.* **1373:** 27–36.
26. Sheffield, M. J., B. L. Baker, D. Li, N. L. Owen, M. L. Baker, and J. D. Bell. 1995. Enhancement of Agkistrodon piscivorus piscivorus venom phospholipase A2 activity toward phosphatidylcholine vesi-

cles by lysolecithin and palmitic acid: studies with fluorescent probes of membrane structure. *Biochemistry.* **34:** 7796–7806.
27. Tatulian, S. A. 2001. Toward understanding interfacial activation of secretory Phospholipase A_2 (PLA_2): membrane surface properties and membrane-induced structural changes in the enzyme contribute synergistically to PLA_2 activation. *Biophys. J.* **80:** 789–800.
28. Høyrup, P., O. G. Mouritsen, and K. Jorgensen. 2001. Phospholipase A(2) activity towards vesicles of DPPC and DMPC-DSPC containing small amounts of SMPC. *Biochim. Biophys. Acta.* **1515:** 133–143.
29. Burack, W. R., A. R. Dibble, M. M. Allietta, and R. L. Biltonen. 1997. Changes in vesicle morphology induced by lateral phase separation modulate phospholipase A2 activity. *Biochemistry.* **36:** 10551–10557.
30. Callisen, T. H., and Y. Talmon. 1998. Direct imaging by cryo-TEM shows membrane break-up by phospholipase A2 enzymatic activity. *Biochemistry.* **37:** 10987–10993.
31. Bartlett, G. R. 1959. Phosphorous assay in column chromatography. *J. Biol. Chem.* **234:** 466–468.
32. Ludescher, R. D., I. D. Johnson, J. J. Volverk, G. H. de Haas, P. C. Jost, and B. S. Hudson. 1988. Rotational dynamics of the single tryptophan of porcine pancreatic phospholipase A2, its zymogen, and an enzyme/micelle complex. A steady-state and time-resolved anisotropy study. *Biochemistry.* **27:** 6618–6628.
33. Parasassi, T., G. De Stasio, A. D'Ubaldo, and E. Gratton. 1990. Phase fluctuation in phospholipid membranes revealed by Laurdan fluorescence. *Biophys. J.* **57:** 1179–1186.
34. Parasassi, T., G. De Stasio, G. Ravagnan, R. M. Rusch, and E. Gratton. 1991. Quantitation of lipid phases in phospholipid vesicles by the generalized polarization of Laurdan fluorescence. *Biophys. J.* **60:** 179–189.
35. Krasnowska, E. K., E. Gratton, and T. Parasassi. 1998. Prodan as a membrane surface fluorescence probe: partitioning between water and phospholipid phases. *Biophys. J.* **74:** 1984–1993.
36. Mariani, P., V. Luzzati, and H. Delacroix. 1988. Cubic phases of lipid-containing systems. Structure analysis and biological implications. *J. Mol. Biol.* **204:** 165–189.
37. Luzzati, V. 1968. X-ray diffraction studies of lipid-water systems. *In* Biological Membranes. D. Chapman and F. H. Wallah, editors. Academic Press, London. 21–123.
38. Parasassi, T., M. Loiero, M. Raimondi, G. Ravagnan, and E. Gratton. 1994. Absence of lipid gel-phase domains in seven mammalian cell lines and in four primary cell types. *Biochim. Biophys. Acta.* **1153:** 143–154.
39. Parente, R. A., and B. R. Lentz. 1984. Phase behaviour of large unilamellar vesicles composed of synthetic phospholipids. *Biochemistry.* **23:** 2353–2362.
40. Lichtemberg, D., M. Menashe, S. Donaldson, and R. L. Biltonen. 1984. Thermodynamic characterization of the pretransition of unilamellar dipalmitoyl.phosphatidylcholine vesicles. *Lipids.* **19:** 395–400.
41. Hønger, T., K. Jørgensen, D. Stokes, R. L. Biltonen, and O. G. Mouritsen. 1997. Phospholipase A2 activity and physical properties of lipid-bilayer substrates. *Methods Enzymol.* **286:** 168–190.
42. Chong, P. L. G., and P. T. T. Wong. 1993. Interactions of Laurdan with phosphatidylcholine liposomes: a high pressure FTIR study. *Biochim. Biophys. Acta.* **1149:** 260–266.
43. Chong, P. L. G. 1988. Effects of hydrostatic pressure on the location of PRODAN in lipid bilayers and cellular membranes. *Biochemistry.* **27:** 399–404.
44. Janiak, M. J., D. M. Small, and G. G. Shipley. 1976. Nature of the Thermal pretransition of synthetic phospholipids: dimyristolyl- and dipalmitoyllecithin. *Biochemistry.* **15:** 4575–4580.
45. Tardieu, A., V. Luzzati, and F. C. Reman. 1973. Structure and polymorphism of the hydrocarbon chains of lipids: a study of lecithin-water phases. *J. Mol. Biol.* **75:** 711–733.
46. Colotto, A., P. Mariani, M. G. Ponzi Bossi, F. Rustichelli, G. Albertini, and L. Q. Amaral. 1992. Lipid-drug interaction: a structural analysis of pindolol effects on model membranes. *Biochim. Biophys. Acta.* **1107:** 165–174.
47. Albertini, G., E. Bertoli, G. Curatola, P. Mariani, F. Rustichelli, and G. Zolese. 1989. Lipid-aminoacid interactions: a study of tryptophan effects on dipalmitoyl-phospahtidylcholine multilamellar liposomes. *Chem. Phys. Lipids.* **50:** 143–153.
48. Jain, M. K., W. Yuan, and M. H. Gelb. 1989. Competitive inhibition of phospholipase A2 in vesicles. *Biochemistry.* **28:** 4135–4139.
49. Carrier, D., M. B. Khalil, and A. Kealey. 1998. Modulation of Phospholipase A_2 by aminoglycosides and daptomycin: a Fourier transform infrared spectroscopic study. *Biochemistry.* **37:** 7589–7597.
50. Grandbois, M., H. Clausen-Schumann, and H. Gaub. 1998. Atomic force microscope imaging of phospholipid bilayer degradation by Phospholipase A_2. *Biophys. J.* **74:** 2398–2404.
51. Nielsen, L. K., J. Risbo, T. H. Callisen, and T. Bjørnholm. 1999. Lag-burst kinetics in Phospholipase A_2 hydrolysis of DPPC bilayers visualized by atomic force microscopy. *Biochim. Biophys. Acta.* **1420:** 266–271.
52. Dennis, E. A. 2000. Phospholipase A_2 in eicosanoid generation. *Am. J. Respir. Crit. Care Med.* **161:** 532–535.
53. Ramirez, F., and M. K. Jain. 1991. Phospholipase A2 at the bilayer interface. *Proteins.* **9:** 229–239.
54. Mustonen, P., J. Y. Lehtonen, and P. K. Kinnunen. 1998. Binding of quinacrine to acidic phospholipids and pancreatic phospholipase A2. Effects on the catalytic activity of the enzyme. *Biochemistry.* **37:** 12051–12057.
55. Chang T-M., C. H. Chang, D. R.Wagner,and W. Y. Chey. 1999. Porcine pancreatic phospholipase A2 stimulates secretin release from secretin-producing cells. *J. Biol. Chem.* **274:** 10758–10764.
56. Mazereeuw-Hautier, J., D. Redoules, R. Tarroux, M. Charveron, J. P. Salles, M. F. Simon, I. Cerutti, M. F. Assalit, Y. Gall, J. L. Bonafe, and H. Chap. 2000. Identification of pancreatic type I secreted phospholipase A2 in human epidermis and its determination by tape stripping. *Br. J. Dermatol.* **142:** 424–431.
57. Flesch, F. M., and B. M. Gadella. 2000. Dynamics of the mammalian sperm plasma membrane in the process of fertilization. *Biochim. Biophys. Acta.* **1469:** 197–235.
58. Ramakrishnan, M., V. Sheeba, S. S. Komath, and M. J. Swamy. 1997. Differential scanning calorimetric studies on the thermotropic phase transitions of dry and hydrated forms of *N*-acylethanolamines of even chain lengths. *Biochim. Biophys. Acta.* **1329:** 302–310.
59. Ueda, I., and T. Yoshida. 1999. Hydration of lipid membranes and the action mechanisms of anesthetics and alcohols. *Chem. Phys. Lipids.* **101:** 65–95.
60. Yuan, C., and M-D. Tsai. 1999. Pancreatic phospholipase A_2: new views on old issues. *Biochim. Biophys. Acta.* **1441:** 215–222.
61. Suezaki, Y., H. Kamaya, and I. Ueda. 1985. Molecular origin of biphasic response of main-phase transition temperature of phospholipid membranes to long chain alcohols. *Biochim. Biophys. Acta.* **818:** 31–37.
62. Laverman, P., M. G. Carstens, O. C. Boerman, E. T. M. Dams, W. J. G. Oyen, N. Van Rooijen, F. H. M. Corstens, and G. Storm. 2001. Factors affecting the accelerated blood clearance of polyethylene glycol-liposomes upon repeated injection. *J. Pharmacol. Exper. Therap.* **298:** 607–612.
63. Vermehren, C., T. Kielber, I. Hylander, T. H. Callisen, and K. Jørgensen. 1998. Increase in phospholipase A_2 activity towards lipopolymer-containing liposomes. *Biochim. Biophys. Acta.* **1373:** 27–36.
64. Abe, T., K. Sakamoto, H. Kamohara, Y. Hirano, N. Kuwahara and M. Ogawa. 1997. Group II phospholipases A_2 is increased in peritoneal and pleuraleffusions in patients with various types of cancer. *Int. J. Cancer (Pred. Oncol.).***74:** 245–250.
65. Jørgensen, K., C. Vermehren, and O. G. Mouritsen.1999. Enhancement of phospholipase A_2 catalysed degradation of polymer grafted PEG-liposomes: effect of lipopolymer concentration and chain length. *Pharm. Res.* **16:** 1493–1495.